

Probing orbital symmetries and ionization dynamics of simple molecules with femtosecond laser pulses

C. D. Lin, and X. M. Tong

J. R. Macdonald Laboratory, Physics Department,
Kansas State University, Manhattan, Kansas 66506-2604, USA

Abstract

It is shown that by measuring the angular distributions of fragmented ions of simple molecules by sub-10 fs laser pulses at intensities in the non-sequential double ionization regime the electron density of the highest occupied molecular orbital can be probed directly. It is also shown that using a single laser pulse, from the kinetic energy release of the fragmented ions following the double ionization of H_2 , the time interval between the two ionizations can be controlled and determined to sub-fs accuracy by varying the pulse duration and laser intensity. Furthermore, using a pump-probe scheme the time evolution of the vibrational wave packet on two potential surfaces can be mapped directly using two sub-10 fs lasers. Theoretical models are used to explain these recent experiments.

1 Introduction

The production of ultra-short optical pulses has opened up an exciting new chapter in the study of molecular dynamics in the last two decades. The wide availability of laser pulses of durations of fractions of picosecond and intensity of the order of 10^{11} W/cm² since the 1990's has lead experimentalists to study the molecules' external degrees of freedom such as their orientation in space, or their center-of-mass motion. Such control of molecules offers many new opportunities in the study of stereodynamical effect in chemical reactions and in gas-surface research. In the last decade, continuing development of laser technology has pushed laser pulses of durations to tens of femtoseconds. Similarly, laser intensity of the order of 10^{14} W/cm² or more are routinely available in most laboratories these days. Within the last few years, new pulse compression technology has made pulses to as short as 5 fs or 4 fs. For such short few-cycle pulses the stabilization and characterization of the carrier-envelope phase is essential, especially in connection with the generation and characterization of attosecond XUV or soft-X-ray pulses.

In this article, we will review some recent progress from the study of simple molecules with femtosecond laser pulses, especially for pulses with duration in the tens to sub-ten femtoseconds, and peak intensity in the range of 10^{13} - 10^{15} W/cm². Our goal is not to offer a comprehensive review of this field. Rather, we would select a few highlights where interesting laser-molecule interaction dynamics have been extracted from experimental results and the results have been quantitatively explained by theoretical calculations. Since direct solution of the time-dependent Schrödinger equation for molecular systems in a laser field under

realistic experimental conditions is not practical, theoretical calculations have to be based on some simple models. It is through this close check-and-balance between experiments and theories that our understanding of the dynamics of the interaction of simple molecules with short laser pulses has emerged.

We have chosen three subjects that we will cover in this article:

- (1) We will show that with proper choice of laser intensity and pulse duration, it is possible to map out directly the electron density distribution of the highest occupied molecular orbital (HOMO) from the angular distributions of the atomic ions following the double ionization of molecules by a sub-10 fs laser.
- (2) We will show that by measuring the kinetic energy release of the fragmented ions from the double ionization of H_2 or D_2 molecules, it is possible to measure the time between the two ionizations to sub-femtosecond precision by a single femtosecond laser pulse. In other words, the molecular clock can be read to sub-fs accuracy using a single laser pulse. The time is measured directly with respect to the optical period of the laser (2.6 fs for 800 nm Ti-Sapphire laser), not its pulse duration. By changing the laser intensity and/or pulse duration one can control the time interval between the two ionizations.
- (3) We will show that in a pump-probe arrangement, the motion of the vibrational wave packet on two potential surfaces can be probed directly. The initial pump pulse is used to ionize the molecule and to create a vibrational wave packet. The time evolution of the vibrational wave packet is probed by further ionization with another laser pulse. By varying the time delay between the two pulses, the vibrational wave packet is mapped from the kinetic energy release of the fragmented ions. For H_2 and D_2 molecules, the motion of the wave packets is shown to be highly nonclassical.

Experimentally the angular distributions and the kinetic energy release of the fragmented ions are determined using the COLTRIMS apparatus [1, 2] where the momentum vectors of the ion fragments are determined at 4π angles simultaneously. The momentum vectors are used to reconstruct the double ionization events. Theoretically, double ionization of molecules leading to the fragmentation is simulated with simple models, by focusing on the different “mechanisms”, and by tracing the time development of the molecule during and after the interaction with laser. Depending on the laser intensity and pulse duration, double ionization can proceed either by sequential double ionization or rescattering double ionization. In the former, double ionizations occur through two successive interactions between the laser’s electric field and the electrons. In the rescattering double ionization, the first ionization occurs through laser-electron interaction. This electron is then driven in the laser field and returns to ionize and remove another electron from the ion. Since the electric field of the laser reaches maximum at each half optical cycle and the electron returning to the ion occurs at well-defined times, double ionization dynamics offers an opportunity to measure the time interval between the two ionizations, in terms of the

optical period of the laser. This is different from the conventional pump-probe experiments where the time interval is limited by the duration of each pulse. To do the theoretical simulation, it is essential that there is a simple theory to calculate the ionization rate of molecules at any internuclear separations. For the rescattering process, the impact ionization cross sections of the molecular ions by the returning electron are also needed. The time evolution of the electron wave packet and the vibrational wave packet of the molecular ion has to be followed as well in the simulation. Since the molecules are randomly distributed, the alignment of the molecules with respect to the laser polarization direction also has to be considered. Our goal in this review is to address all the elements used in such theoretical simulations. By comparing the theoretical results with experiments, we learned how to understand and how to control the breakup of molecules under intense laser fields.

In Section 2 we first discuss the simple tunneling ionization theory of molecules by lasers, including its alignment dependence. This theory, with additional assumptions which are valid for short sub-10 fs laser pulses, is used to show that the angular distributions of the double ionization fragments of diatomic molecules directly mimic the electron density distributions of the highest occupied molecular orbitals. In Section 3 we show how to read the molecular clocks to sub-fs accuracy using the double ionization of H_2 and D_2 molecules. The time evolution of the vibrational wave packet on two potential surfaces is examined in Section 4 for H_2^+ and D_2^+ ions theoretically — showing their highly non-classical behavior. It is shown that these wave packets can be probed directly by further ionizing the molecular ions after a time delay and by measuring the energies of the fragmented ions. The experimental results are then shown to be in agreement with theoretical simulations.

2 Probing molecular orbital symmetry with sub-10 fs laser pulses

When neutral molecules are subjected to intense laser fields they can undergo single or multiple ionizations, followed possibly by immediate dissociations. Many experiments [3, 4, 5] since 1990's have shown that the ionized fragments are strongly forward peaked in the direction of the laser polarization. The nature and the mechanism leading to such strong anisotropic angular distributions have been rather unclear. In general one can expect that ionization rates of molecules depend on the alignment and/or orientation of the molecular axis with respect to the laser polarization direction, but it is also well known that molecules can be aligned by the laser field [6]. Typically the time it takes to align molecules is of the order of fractions to tens of picoseconds, but experiments using lasers with pulse durations of a few tens of femtoseconds still showed strong forward peaking in the fragment's angular distributions. This has been taken to imply that all molecules are favorably ionized when their molecular axis is aligned with the laser polarization direction. However, re-

cent experiments [7, 8, 9, 10] with laser pulses of duration of less than 10 fs showed that this conclusion is not correct. For such short pulses the angular distributions of the fragments are not always forward peaked. In fact, the experimental angular distributions are in agreement with the alignment-dependence predicted by the recently developed molecular tunneling ionization theory [11]. This theory shows that the alignment-dependent ionization rates of molecules are determined predominantly by the orbital symmetries of the highest occupied molecular orbital (HOMO). In these experiments, it has also been shown that the angular distributions are strongly forward peaked if the laser pulses have durations in the tens of femtoseconds, or for the sub-10fs pulses when the laser intensity is higher. The latter results have now been attributed to the post-ionization alignment (PIA) effect by Tong *et al.* [9]. For lasers of durations of several tens of femtoseconds, the molecules are hardly aligned by the pulse. However, for such pulses each molecule acquires enough angular momentum (or angular velocity) before ionization. When such a rotating molecule breaks apart by Coulomb explosion, each fragment would rotate an additional angle toward the polarization axis direction before they come to stop. This PIA effect has been shown to be most effective in aligning the fragmented ions in the laser polarization direction. Thus to extract alignment-dependent tunneling ionization rates from the angular distributions of fragmented ions, laser pulses of sub-10 fs durations and moderate intensity are needed. We first summarize the molecular tunneling ionization theory.

2.1 Molecular tunneling ionization theory

The tunneling ionization theory for atomic hydrogen by a static electric field is a standard textbook subject in quantum mechanics [12]. In the version for the tunneling ionization of atoms by laser fields, in the so-called ADK (Ammosov-Delone-Krainov) model [13], the ionization rate has been given analytically. For tunneling ionization, besides the barrier penetration probability, the rate is proportional to the electron density at the far region near the top of the potential barrier (from the combined Coulomb potential and the static field potential). Since the electronic charge density in a molecule is not isotropic it is clear that the ionization rates of molecules in an intense laser field will depend on the alignment of the molecules. For many years such alignment dependence cannot be readily evaluated theoretically until the molecular tunneling ionization theory (MO-ADK) [11] was developed. The ionization rates of molecules are also given analytically according to the MO-ADK theory. It further predicts simple alignment dependence of the ionization rates.

For an atom, the wavefunction of the valence electron at large distance where tunneling occurs can be written as

$$\Psi^m(\mathbf{r}) = C_l F_l(r) Y_{lm}(\hat{\mathbf{r}}), \quad (1)$$

where

$$F_l(r \rightarrow \infty) \approx r^{Z_c/\kappa - 1} e^{-\kappa r}, \quad (2)$$

with Z_c the effective Coulomb charge, $\kappa = \sqrt{2I_p}$, and I_p is the ionization energy. The $Y_{lm}(\hat{\mathbf{r}})$ is the usual spherical harmonics. These expressions are for an electron with angular momentum quantum numbers ℓ and m . For molecules, the electronic wavefunction is multi-center in nature. To employ the ADK formula directly, one needs to expand the wavefunction in the asymptotic region in terms of one-center expressions. Thus one writes the molecular wavefunction in the asymptotic region as

$$\Psi^m(\mathbf{r}) = \sum_l C_l F_l(r) Y_{lm}(\hat{\mathbf{r}}), \quad (3)$$

where the summation over ℓ is needed. The quantization axis in this case is along the internuclear axis and $|m|$ is a good quantum number. The coefficients C_l are obtained by fitting the asymptotic molecular wavefunction calculated from other quantum chemistry codes in the form of equation (3). The coefficients depend on the internuclear separation and on the electronic state. For molecules at or near the equilibrium distance, only a few partial waves will be needed in the summation. Once the coefficients C_l are available the ionization rate for a diatomic molecule with its axis aligned with the laser polarization is given by

$$w_{stat}(F, 0) = \frac{B^2(m)}{2^{|m|} |m|!} \frac{1}{\kappa^{2Z_c/\kappa-1}} \left(\frac{2\kappa^3}{F} \right)^{2Z_c/\kappa-|m|-1} e^{-2\kappa^3/3F}, \quad (4)$$

where

$$B(m) = \sum_l C_l Q(l, m), \quad (5)$$

and

$$Q(l, m) = (-1)^m \sqrt{\frac{(2l+1)(l+|m|)!}{2(l-|m|)!}}. \quad (6)$$

Clearly the factor $B^2(m)$ contains all the information about the electron density in the tunneling region along the direction of the electric field. For electrons in the σ orbitals the electron density is large along the molecular axis. Thus ionization rates will be large if the molecular axis is aligned in the direction of the laser polarization. For molecules which have outermost electrons in π orbitals, the electron density along the molecular axis vanishes, such that tunneling ionization rates would be zero if the molecular axis is aligned in the laser polarization direction. This is the most transparent consequence of tunneling ionization theory for molecules in a laser field.

If the molecular axis is not aligned along the field direction, but at an arbitrary angle \mathbf{R} with respect to it, then the $B(m)$ in Eq. (4) is obtained through a rotation, and is expressed as

$$B(m') = \sum_l C_l D_{m',m}^l(\mathbf{R}) Q(l, m'), \quad (7)$$

with $D_{m',m}^l(\mathbf{R})$ being the rotation matrix and \mathbf{R} the Euler angles between the molecular axis and the field direction. The static field ionization rate is

$$w_{stat}(F, \mathbf{R}) = \sum_{m'} \frac{B^2(m')}{2^{|m'|} |m'|!} \frac{1}{\kappa^{2Z_c/\kappa-1}} \left(\frac{2\kappa^3}{F} \right)^{2Z_c/\kappa-|m'|-1} e^{-2\kappa^3/3F}. \quad (8)$$

The ionization rate in a low frequency laser field is obtained by averaging the rates over an optical cycle and is given by

$$w(F, \mathbf{R}) = \left(\frac{3F}{\pi\kappa^3} \right)^{1/2} w_{stat}(F, \mathbf{R}). \quad (9)$$

where F now stands for the peak field strength.

An immediate direct consequence of the MO-ADK theory is that the ionization rates for any space-fixed molecules are proportional to the electron density in the direction of the laser polarization direction. In other words, by measuring the alignment dependence of the ionization rates, the electron density of the outermost molecular orbital can be directly probed. This is the most significant prediction of the MO-ADK theory.

2.2 Alignment dependence of tunneling ionization rates and the symmetry of molecular orbitals

How can one extract the alignment dependent ionization rates of molecules experimentally? Neutral molecules are not easily aligned by external fields. The angular distributions of singly charged molecular ions after single ionization by a laser pulse are not easily determined due to their small recoil momenta. To measure the orientation of the molecule, or more precisely, the direction of the molecule at the time of ionization, it is most convenient if the ionized molecules break up into two fragmented ions, where the events are clearly identified by their momenta adding up to zero. Such techniques are routinely employed in experiments using COLTRIMS apparatus where the momentum of each individual fragmented ion is measured over 4π angles.

In order to extract the alignment-dependent ionization rates of molecules from such double ionization experiments, additional conditions must be met. First, the laser pulses should not align the molecules before ionization, and that the axis between the two fragmented ions does not entail additional rotation during the breakup process. In other words, there is no adiabatic alignment before the ionization, and the post-ionization alignment effect (PIA) can be neglected. Both effects have been considered theoretically in Tong *et al.* [9] and it was concluded that these aligning factors become negligible by going to a short pulse of sub-10 fs duration with moderate intensity (say near or below 10^{14} W/cm²).

In the experiments, since the molecules are doubly ionized by the laser pulse, it is advantageous to choose laser parameters such that the second ionization is isotropic or nearly isotropic with respect to the orientation of the molecules.

This is accomplished by using lasers with intensity in the nonsequential double ionization regime. For such processes, the first ionization is by tunneling, and the second ionization is due to the electron impact excitation or ionization by the tunneling ionized electron which has been driven back to collide with the molecular ion by the laser fields. By choosing relatively weak laser intensity with sub-10 fs durations, such experiments have been carried out recently at Kansas State University [7, 8, 9, 10] for a number of molecules. The angular distributions of the fragmented ions give directly the alignment dependence of the ionization rates which can be compared to the prediction of the MO-ADK theory.

In Fig. 1 we show the angular distributions of the fragmented ions from double ionization by a linear polarized laser [7, 8, 9, 10] and the comparison with the alignment dependence of the tunneling ionization rates predicted by the MO-ADK theory. Shown are the results for N_2 , O_2 , CO , CO_2 and C_2H_2 . For CO_2 , the breakup channel considered was $\text{CO}_2^{2+} \rightarrow \text{CO}^+ + \text{O}^+$. For $\text{C}_2\text{H}_2^{2+}$, it is the fragmentation into two CH^+ ions. These distributions are compared to the alignment-dependent ionization rates of molecules using the MO-ADK theory (2nd column) and with the density distributions of the molecular orbitals (3rd column) from which the electrons have been ionized. The molecular orbitals were calculated from the GAMESS code [14] for molecules at their equilibrium distances and the calculated electronic wavefunctions were visualized by the MOLEKEL program [15].

In Fig. 1 the angular distributions for N_2 and CO are quite similar. The HOMO of N_2 has σ_g symmetry and of CO has σ symmetry, and their angular distributions are peaked in the direction of the laser polarization, in agreement with the fact that the electron density for σ_g (or σ) orbital peaks in the direction of the internuclear axis. (The experiments cannot separate C–O from O–C in the sample so their angular distribution is symmetric.)

In Fig. 1 we also note that the angular distributions for O_2 and CO_2 are very similar. Their angular distributions peak away from the laser polarization direction. The HOMO of each molecule has π_g symmetry, and according to the MO-ADK theory the ionization rate peaks when the molecules are aligned at an angle of about 40° for O_2 and 25° for CO_2 , respectively. The latter has a smaller angle because of the larger O–O bond length. The ionization rates show a minimum in the laser polarization direction instead of zero as would be expected for a pure π_g orbital, reflecting the approximate nature of the pure MO description of the HOMO orbital for wavefunctions in the asymptotic region.

In Fig. 1 the angular distributions of C_2H_2 are also shown. For C_2H_2 , its HOMO has the π_u symmetry. Again, the angular distributions measured are in good agreement with the prediction of the MO-ADK theory and with the symmetry property of the π_u orbital.

The results shown in Fig. 1 clearly indicate that the measurement of alignment dependence of tunneling ionization rates provides an experimental verification of the “physical reality” of molecular orbitals (MO). The MO is often considered as a mathematical construct. Its utility is tied closely to the validity of the shell model or the Hartree-Fock approximation for the ground state of

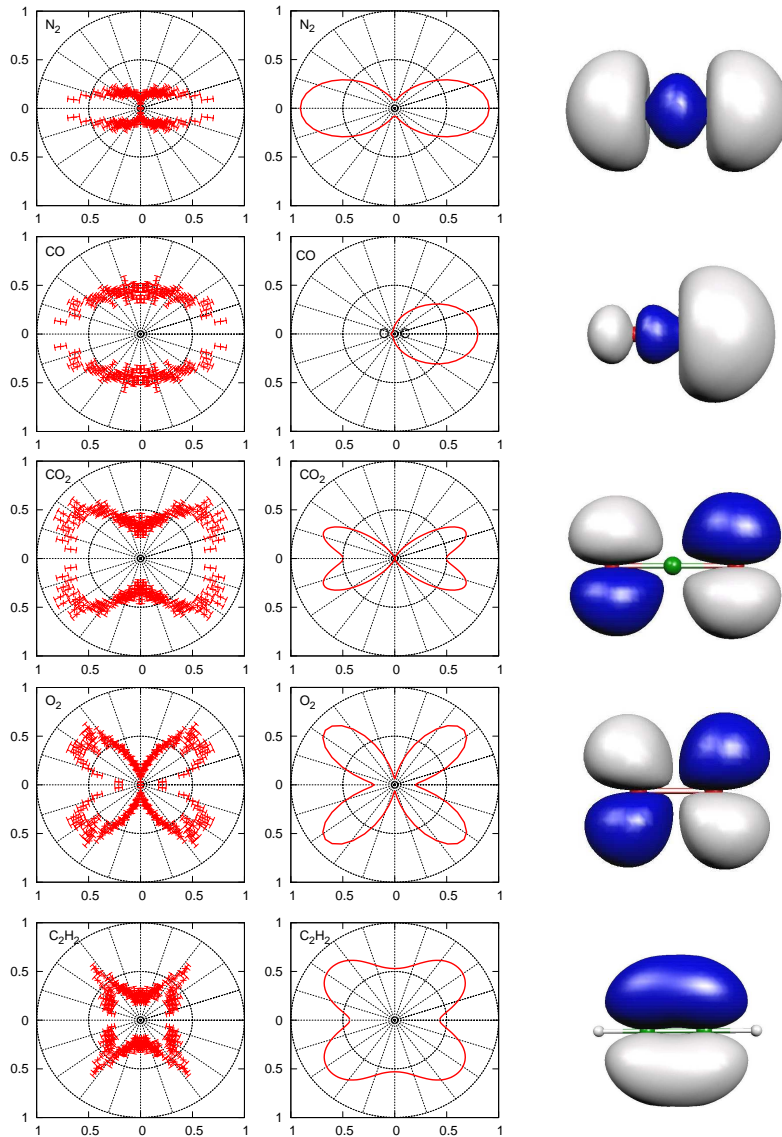


Figure 1: Comparison of the measured angular distributions of the fragmented ions of the double ionization of molecules (first column) with the alignment-dependent tunneling ionization rates predicted by the MO-ADK theory (second column) for N_2 , CO , CO_2 , O_2 and C_2H_2 , respectively. For each molecule, the laser intensity was chosen in the nonsequential double ionization regime where the second ionization is by electron impact ionization. Sub-10 fs laser pulses are used to avoid additional alignments that modify the measured angular distributions. The corresponding highest occupied molecular orbital for each molecule is also plotted (third column). Experimental data are taken from Refs. [7, 8, 10].

molecules. Granted that the results of Fig. 1 only provide the density distributions. However, the approximate nodal planes can be identified from the measured angular distributions such that wavefunctions can be deduced. We note that in most quantum measurements the signal is proportional to the square of the matrix element of an operator taken between the initial and the final states. Thus it is often difficult to unravel from the measured angular distributions the geometric effect of the initial state and the final state separately. For tunneling ionization of molecules, ionization occurs primarily from electrons initially in the direction of the electric field. In the tunneling process by linearly polarized light the ionized electrons remain in the direction of the electric field. By measuring the breakup of the molecular ion thus gives a direct measurement of the electron density distribution of the outermost orbital if the molecular axis does not undergo additional rotation in the breakup process. These conditions are met for non-sequential double ionization of simple molecules by sub-10 fs laser pulses.

Before closing we stress that the use of sub-10 fs laser pulses with relative low laser peak intensity is essential to guarantee that the molecules are not aligned by the lasers before the ionization, nor that the axis of the fragmented ions are rotated in the breakup process. In Fig. 2 we show the comparison of the angular distributions of the nonsequential double ionization of O_2 by 8 fs and 35 fs pulses at peak intensity of 2.0×10^{14} W/cm² and 2.2×10^{14} W/cm², respectively [9]. The experimental angular distributions of the O^+ ions are shown on the right. On the left theoretical calculated angular distributions are shown. In the figure, $R(\theta)$ is the angular distribution from the MO-ADK theory alone, $S_0(\theta)$ is the angular distribution predicted by including the alignment of the neutral molecules before ionization, assuming that the molecules are ionized at the peak of the laser pulse. For both pulses, this alignment is insignificant. In the figure, the angular distributions $S_f(\theta)$ are also shown. In this case, post-ionization alignment effect is included. Recall PIA accounts for the additional rotation of the axis of the fragment ions during the breakup process. This effect is small for the 8 fs pulse but significant for the 35 fs pulse. The inclusion of the PIA effect explains why the fragmented ions are strongly forward peaked in the laser polarization direction. For the 35 fs pulse, even though it does not have time to align the molecules significantly, the laser does impart enough angular momentum to each molecule. The PIA is the result of the additional rotation of the molecular axis during the breakup process.

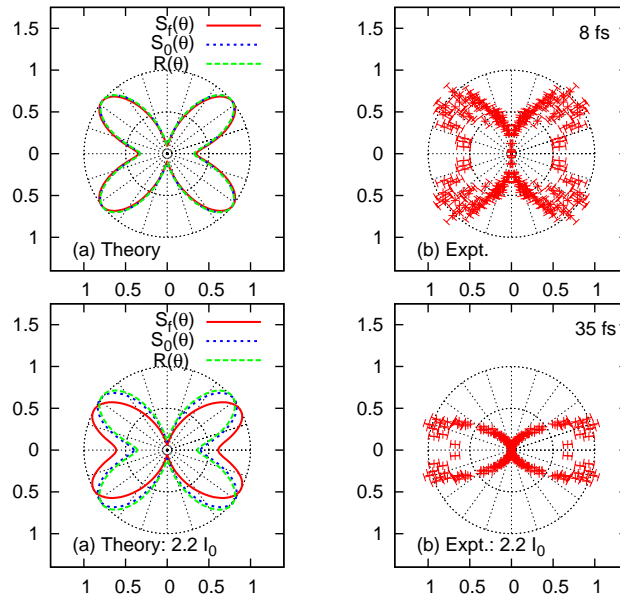


Figure 2: (upper panel) Comparison of the simulated angular distributions of the fragmented O^+ ions for an 8 fs laser pulse at peak intensity of $2.0 \times 10^{14} \text{ W/cm}^2$. $R(\theta)$ is the alignment-dependent ionization signal calculated from MO-ADK theory; $S_0(\theta)$ is the simulated angular distributions calculated including the effect of adiabatic alignment before molecules are ionized; and $S_f(\theta)$ is the same distribution including additional effect from post-ionization alignment(PIA). (lower panel) Same as above but for a 35 fs laser pulse at peak intensity of $2.2 \times 10^{14} \text{ W/cm}^2$.

3 Attosecond molecular clocks: Time-resolved double ionization dynamics of H_2 and D_2 molecules

3.1 Dynamics of double ionization of H_2 by femtosecond lasers

Since the advent of femtosecond lasers, femtochemistry has become possible where chemical reaction dynamics can be probed at the atomic time scale [16]. Pump-probe experiments have been widely used to study the rotational and vibrational wave packets in the presence of laser pulses of durations of tens or hundreds of femtoseconds. Clearly femtosecond laser pulses are not suitable for measuring or controlling the vibrational motion of simple molecules like H_2 or D_2 which have vibrational periods of about 14 fs and 20 fs, respectively. Recently, however, following the initial suggestion of Corkum and coworkers [17, 18], it has been shown that it is possible to make time-resolved measurements

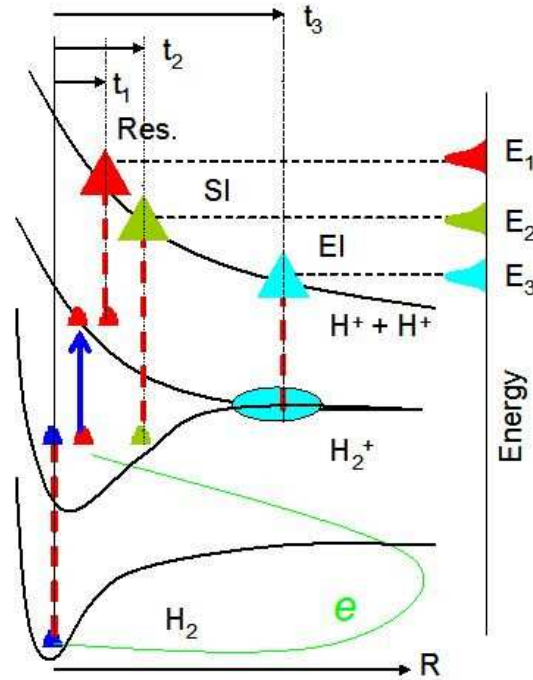


Figure 3: Schematic of different processes leading to the double ionization of H_2 molecules in an intense laser field.

of the fragmentation of H_2 molecules (our discussions will directly refer to H_2 even though the same description can be used for D_2 as well.) using lasers of durations of tens of femtoseconds. The time can be read with the precision of attoseconds, or more precisely, at sub-femtoseconds, using the concept of a molecular clock which ticks with the period of the optical cycle of the laser. The clock is “started” by the first ionization and “stopped” by the second ionization. In this approach, the kinetic energy release of the measured fragments is used to read the internuclear distance of the wave packet as a function of time which is triggered only after the first ionization. By changing the laser intensity, the mean wavelength of the laser, and/or the pulse duration, the time interval between the two ionizations can be read and can be controlled.

Double ionization of H_2 molecules by an intense laser can proceed via (1) sequential double ionization (SI); (2) rescattering double ionization (RES) and (3) enhanced ionization (EI). Their relative importance depends on the laser intensity. These processes are depicted schematically in Fig. 3. For the rescattering double ionization, H_2 is first singly ionized near the peak field of an optical cycle. Upon this ionization, the clock begins to tick. This first ionization launches a correlated electron wave packet and a vibrational wave packet. Under the oscillating electric field, the electron released in the first ionization returns to

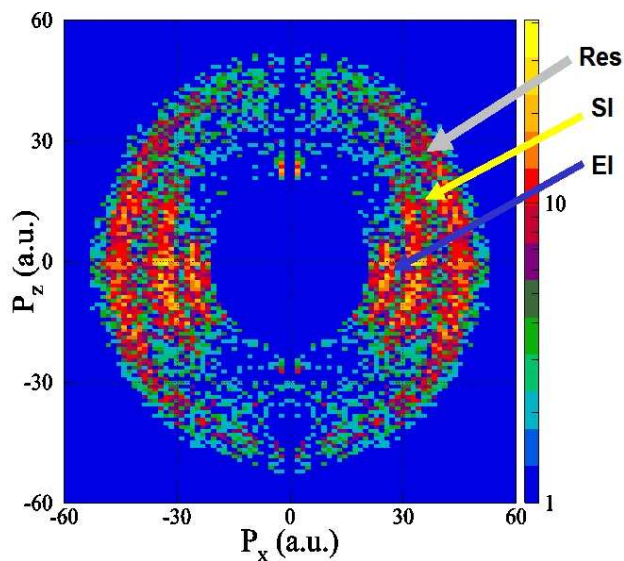


Figure 4: Momentum image of H^+ pairs from the double ionization of H_2 molecules by a laser pulse of intensity $3 \times 10^{14} \text{ W/cm}^2$. The laser polarization is along the x -direction. The image is taken from Ref. [26].

the parent ion at relatively well-defined times, to excite it to the excited electronic states or to ionize it. If the H_2^+ is in the excited electronic state, it can dissociate to $H^+ + H$, or it can be further ionized by the laser when its electric field reaches the peak again. The second ionization leads to $H^+ + H^+$. From the released kinetic energy E_1 , the internuclear separation R where the second ionization occurs can be determined. Since the propagation of the vibrational wave packet in the ground electronic potential curve of H_2^+ is well understood, the time t_1 of the second ionization can be read. In the sequential double ionization, the second ionization occurs at time t_2 when the laser electric field reaches the maximum again. Since tunneling ionization rate depends strongly on the ionization energy, SI tends to occur at larger internuclear distances where the ionization potential is smaller, thus resulting in smaller kinetic energy E_2 . If the H_2^+ is not ionized by RES nor by SI, some part of the vibrational wave packet can reach large internuclear separation where H_2^+ can be ionized by charge resonance enhanced ionization (CREI) [19] or enhanced ionization (EI) in short. The released kinetic energies from the EI process are much smaller and have been extensively studied previously [20, 21, 22, 23, 24, 25]. The EI process occurs in the flat region of the potential curve so that time cannot be accurately read.

By choosing proper laser intensity and duration, all of the three processes can be made to contribute to the double ionization of H_2 . Fig. 4 shows the momentum image of the H^+ pairs produced in the double ionization of H_2 by a 14 fs pulse with peak intensity of $3 \times 10^{14} \text{ W/cm}^2$ as reported by Alnaser *et*

al. [7]. The coexistence of RES, SI and EI for the double ionization of H_2 is clearly seen. Fig. 4 also shows the angular distributions of the two proton pairs. Clearly EI is favored only when the molecules are lying nearly parallel to the laser polarization direction. This is consistent with the fact that CREI is the result of the coupling between the ground σ_g and the excited σ_u electronic states. This coupling requires that the laser polarization and the internuclear axis to be parallel to each other. Fig. 4 also shows that the angular distributions from the rescattering cover a larger range of angles. This shows that the rescattering process is not very sensitive to the alignment of the H_2^+ ion. Since in the RES, the second ionization is triggered by the impact excitation or ionization of the returning electron. This wave packet is sufficiently broad in the transverse direction and the excitation and ionization cross sections are expected to depend weakly on the alignment of the molecules.

3.2 Theory of double ionization of H_2 by femtosecond lasers: Rescattering region

To understand and interpret the time-resolved double ionization dynamics of H_2 molecules in a laser field quantitatively, we have developed a theoretical model that follows the time-evolution of the reaction processes. A more complete schematic diagram of the rescattering processes is given in Fig. 5. On the second row, the time-dependent electric field of the laser is shown. At time t_0 , the H_2 molecule is first ionized from its equilibrium distance. The vibrational wave packet created at this time is sketched on the top row. At t_1 , the ionized electron is driven back to the H_2^+ ion. The electron can excite H_2^+ from the ground electronic state to the excited σ_u or π_u electronic states. Once it is in the excited electronic states, it can dissociate to $H^+ + H$, with the release of total kinetic energy characterizing the wave packet at time t_1 . Or it can be ionized by the laser again a quarter optical cycle later at time t_1' . The resulting doubly charged H_2^{2+} will then Coulomb explode. The two protons can be detected at the end with total kinetic energy release characteristic of the internuclear separation at the time t_1' of the second ionization.

For a femtosecond laser pulse, the rescattering process discussed above occurs within one optical cycle after the first ionization. However, additional processes occur after one optical cycle. At time t_2 , the rescattered electron will revisit the ion core, and similarly at time t_3 . At both times the electron can contribute to the excitation of the molecular ion and the further dissociation or ionization. In the meanwhile, the vibrational wave packet continues to move outward to larger R and the excitation or ionization cross sections have to be calculated from molecular ions at these internuclear distances.

In Tong *et al.* [27, 28], the theoretical model for simulating the kinetic energy release spectra for the rescattering double ionization has been discussed in details. It involves the following steps:

- (1) The ionization rate of H_2 from the equilibrium distance at time t_0 is calculated using the MO-ADK theory. The initial vibrational wave packet

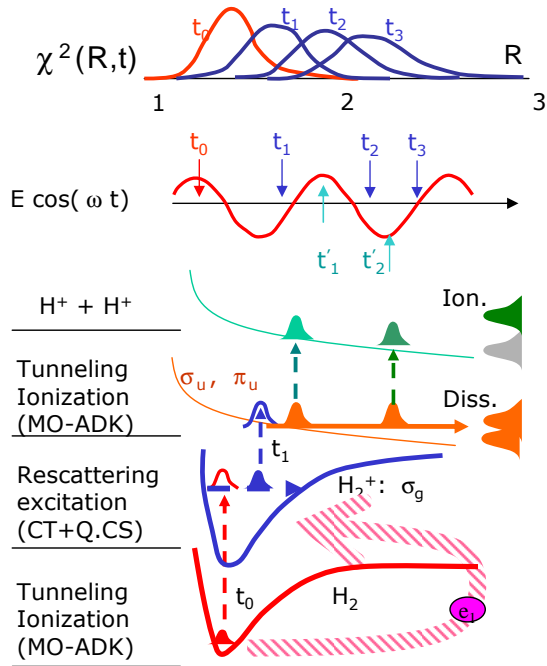


Figure 5: Schematic of the major physical processes leading to the formation of H^+ ion. The H_2 is first ionized at t_0 creating an electron wavepacket which returns to collide with H_2^+ at time t_1 . In the meanwhile the initial vibrational wave packet, measured by $\chi^2(R,t)$, created at t_0 , is shifted to larger R and broadened at later time. At t_1 , the H_2^+ is excited from σ_g to σ_u and π_u by electron impact. The excited H_2^+ can dissociate directly to give H^+ , or can be further ionized at t'_1 , t'_2 , etc to produce two H^+ ions by Coulomb explosion. Note that similar rescattering processes can be initiated at later time, t_2 , t_3 , etc, and are included in the calculated H^+ spectra.

is given by the Frank-Condon principle. It then freely propagates in the ground potential curve of H_2^+ . This propagation leads to wave packet spreading as time goes on.

- (2) The model for describing the motion of the ionized electron in the laser field is similar to the method used by Yudin and Ivanov [29] for He. The electron in the laser field and the Coulomb field of the residual ion is calculated classically by solving Newton's equation of motion. The initial velocity is assumed to have the distribution as given by the ADK model and the electron's initial position is along the polarization axis, at the top of the barrier where ionization starts. The electron's trajectory is calculated for over seven optical cycles (or till when the pulse is over for the short pulses) and the distance of the electron from the ion core is monitored. The time and the kinetic energy when the electron reaches the

distance of closest approach are recorded. From these data, we further extract the equivalent asymptotic scattering energy and impact parameters without the presence of the laser field.

- (3) We next need the electron impact excitation cross sections for H_2^+ from the ground state to the excited $2p\sigma_u$ and $2p\pi_u$ states, for the molecular ion fixed in space and for different internuclear separations. Such elementary cross sections are not available. Since the united-atom limit of H_2^+ is He^+ and the separated-atom limit is $H^+ + H$, we fit the excitation cross sections of H and of He^+ from the close-coupling calculations and scaled the scattering energy in terms of excitation energy. We found that the cross sections for both H and He^+ [30] can be well-fitted with only a few parameters. The fitted excitation cross sections are then used to calculate the excitation cross sections from H_2^+ at different internuclear separations.
- (4) Once the H_2^+ are in the excited states, they can dissociate. Depending on rescattering occurs at $t_1, t_3, ..$ (the contribution from t_2 is always negligible due to its small return energy), the release kinetic energy from the dissociation will be different. If the excited H_2^+ ions are further ionized by the laser, depending on it occurring at $t'_1, t'_2, ..$ etc, the released kinetic energy from the Coulomb explosion will be different.
- (5) Recall that at each time t , the vibrational wave packet has a spread and thus the kinetic energy release will have a spread. The kinetic energy release also depends on which excited electronic state is populated by the excitation process.
- (6) Since the first ionization will occur near the peak of the electric field in an optical cycle, we need to integrate over all the contributions over t_0 near the peak of the field. Since the tunneling ionization rate is strongly dependent on the instantaneous electric field, this integration should cover only a small fraction of a femtosecond near the peak field.

By putting all these calculations together, the kinetic energy release can be obtained. Figure 6 shows the kinetic release of D^+ measured by Niikura *et al.* [17] for a 35 fs pulse at peak intensity of 1.5×10^{14} W/cm². In this experiment, only one D^+ ion is measured. Thus the contribution includes both dissociation and double ionization. The results from the theoretical simulation are shown for three intensities indicated and the results for the three intensities from the theory are normalized at the peak. It shows that the simulation reproduced well the kinetic energy release spectra, particularly at the main peak region.

The theoretical simulation allows us to disentangle the various contributions to the calculated kinetic energy release spectra. This is shown in Fig. 7. We separate contributions occurred within the first cycle or the second cycle after the initial ionization and distinguish D^+ resulting from dissociation or ionization. We clearly see that ionization is much more significant than dissociation and that the main peak in Fig. 6 is the result of double ionization where the

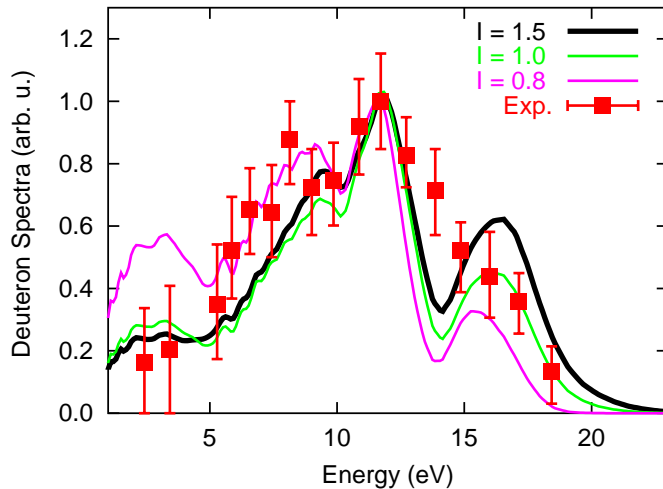


Figure 6: D^+ ion yield at several intensities for a 35 fs laser pulse ionizing D_2 molecules. The experimental data are from Ref. [18] for intensity at $1.5 I_0$, where $I_0=10^{14}$ W/cm 2 . The peak values from the experiment and from the theory for $1.5 I_0$ are normalized to each other. For peak intensities of $1.0 I_0$ and $0.8 I_0$, the yields have been multiplied by 1.4 and 3.0, respectively, to have the same peak ion yield height.

rescattering occurs at near t_3 . A similar simulation showed that dissociation would become more important for laser intensity of 8×10^{13} W/cm 2 .

This comparison demonstrates that to read the molecular clock precisely the mechanism of double ionization of the simple H_2 molecule has to be understood well.

3.3 Control the time sequence of double ionization by tuning laser parameters

From the rescattering theory it is clear that the kinetic energy of the returned electron at the ion core depends on the laser peak intensity, while the relative importance of the first return, the third return, etc, depends on the laser pulse durations. By changing the laser peak intensity and pulse length, the rescattering-induced Coulomb explosion can be controlled. In Fig. 8 we show the experimental KER spectra resulting from double ionization of H_2 by 30 fs pulse with intensity of 0.9×10^{13} and 2.2×10^{13} W/cm 2 . The experimental data [26] are compared to the theoretical calculations [27, 28]. Note that for the higher intensity, the relative contribution from the first return becomes more significant. With the higher intensity the kinetic energy of the returned electron is higher such that electron impact excitation to the excited state at short time or small internuclear separation is possible. By going to the shorter pulse, say, 8 fs, the data [26] shown in Fig. 8 clearly indicate that rescattering from the first

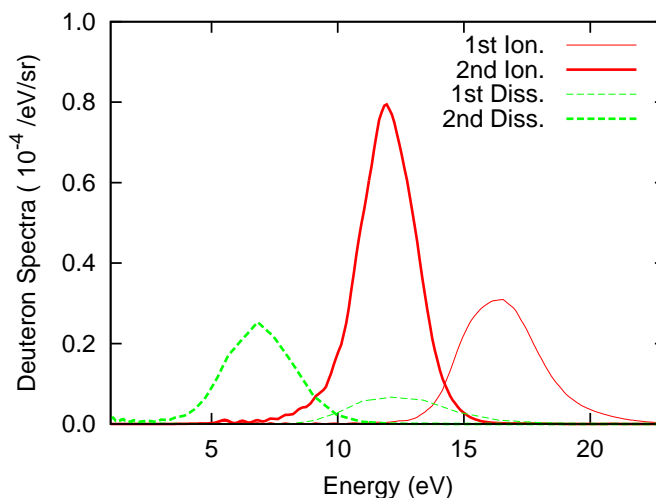


Figure 7: Decomposition of D^+ ion yields into contributions from dissociation and ionization, and for rescattering occurring within the first and the second optical cycle after the initial tunneling ionization. The peak laser intensity is 1.5×10^{14} W/cm² and pulse length is 40 fs.

return is more important. For the short pulse, the electric field of the laser at the third return is already much weaker such that the third return has much less contribution. Thus from the kinetic energy spectra, in the rescattering double ionization regime, the subsequent time for the second ionization by the laser following the first ionization can be controlled by changing the laser intensity. The second ionization occurs at well-specified time, within the first return or the third return. These well-defined return times lead to well-specified internuclear separations at which double ionization occurs, and subsequently, well-defined kinetic energy release. The width of the kinetic energy peaks gives the uncertainty of the time measurements to sub-femtoseconds. They form the basis of the “molecular clocks” where time can be read at sub-femtosecond accuracy. Alternatively, one can also use lasers of different wavelengths. Since the rescattering is measured in terms of the optical period of the laser, by using lasers of different mean wavelengths, the kinetic energy release peaks will shift with the mean wavelength of the laser. This method was used in Niikura *et al.* [18] where the concept of molecular clocks was first reported.

As the laser intensity becomes large, double ionization occurs sequentially [31]. The first electron is ionized at the beginning part of the laser pulse, followed by the second ionization later after the vibrational wave packet has moved to a larger internuclear separation such that further ionization of H_2^+ is possible. Clearly each ionization occurs only when the laser intensity reaches the peak at each half optical cycle. By changing the pulse duration, the time for the laser to reach intensity high enough for the second ionization is longer if the pulse

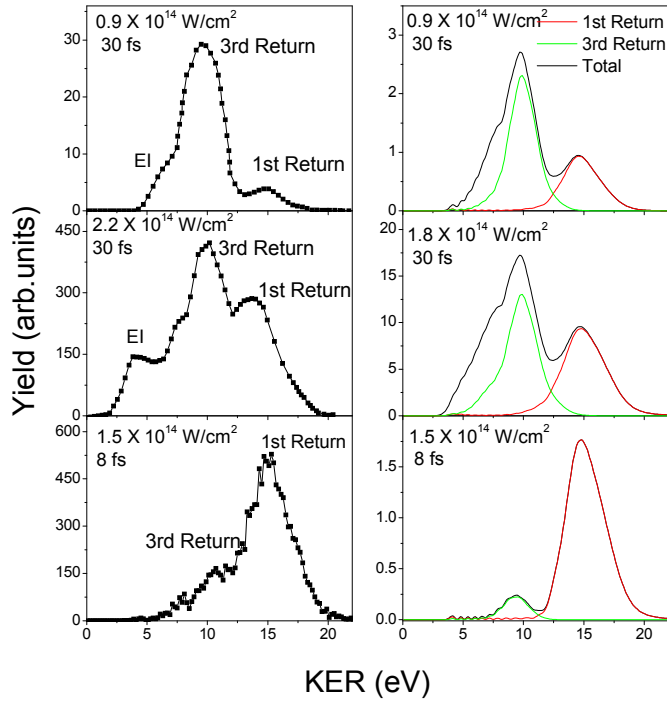


Figure 8: Comparison of the measured rescattering KER spectra of H_2 in 30 and 8 fs laser pulses [26]. The right column shows this comparison as predicted by the Rescattering model [27, 28].

length is longer. Fig. 9 shows the time and the internuclear distance where the second ionization occurs for a laser pulse of duration of 5 fs, 10 fs and 15 fs, for laser of peak intensity of $2.8 \times 10^{15} \text{ W/cm}^2$. In this case, the molecular clock is triggered at the first ionization. For the second ionization, it occurs after one, one-and one-half, and two optical laser cycles later, respectively, for the three pulses listed above. Clearly the kinetic energy release spectra in the sequential double ionization region depend not sensitively with respect to the laser's peak intensity, but the pulse duration is important.

At the higher intensity just discussed, the contribution from the rescattering is negligible. By taking an “intermediate” intensity, both the rescattering and the sequential double ionization can occur and their respective kinetic energy peaks are characterized by the clock for either rescattering or sequential ionization.

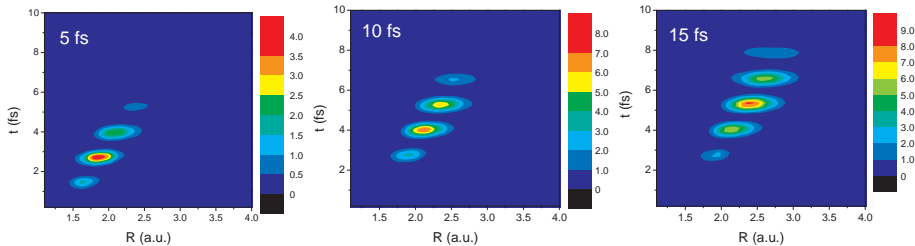


Figure 9: 2D plots of sequential double ionization spectra of D_2 vs time interval after the first ionization and the internuclear separation. The lasers have pulse durations of 5, 10, and 15 fs and peak intensity at 2.8×10^{15} W/cm 2 .

4 Probing nonclassical vibrational wave packets on two potential surfaces

The double ionization dynamics described in the previous section focussed on the laser- H_2^+ interaction following the first ionization of H_2 from its initial equilibrium distance. This initial ionization creates a vibrational wave packet which propagates outward in the σ_g ground potential curve of H_2^+ . Assuming that the Frank-Condon principle applies, this initial wave packet is given by the ground vibrational wavefunction of H_2 . As this wave packet propagates outward, it will be reflected back as it reaches near the outer classical turning point. In an intuitive classical picture, this vibrational wave packet is to oscillate indefinitely between the inner and outer classical turning points. Quantum mechanical calculations, however, show that the wave packet does not behave this way. The wave packet is rather dispersive, and it will spread as it moves in the σ_g ground potential. The electric field from the laser is not important till at large R where the σ_g potential is separated from the upper σ_u curve by about one unit of photon energy. The strong coupling between these two curves is what is responsible for the dissociation of H_2^+ to $H^+ + H$ via bond-softening. Experimentally they are identified by the low energy peaks below 1 eV in the dissociation kinetic energy spectra [32]. In other words, the laser can couple σ_g and σ_u potential curves, and the wave packet which rides only on the lower σ_g curve can now be split into two wave packets after the first encounter in the outer turning point region. Now we ask what happens subsequently to the two wave packets.

From the theoretical point of view, the effect of laser coupling of the two wave packets can be easily calculated by solving the time-dependent wave functions involving the two σ_g and σ_u potential curves by the laser. The modulus square of the two wave packets are shown in Fig. 10 where the density of each wave packet has been displayed vs time. In the model calculation [33], we assumed a Gaussian wave packet of width (FWHM) of 8 fs and the D_2 was ionized initially at the peak of the laser pulse. The tail of the laser pulse couples the two electronic states. For the wave packet riding on the upper repulsive σ_u potential curve, it moves monotonically outward. At large time one can see broadening,

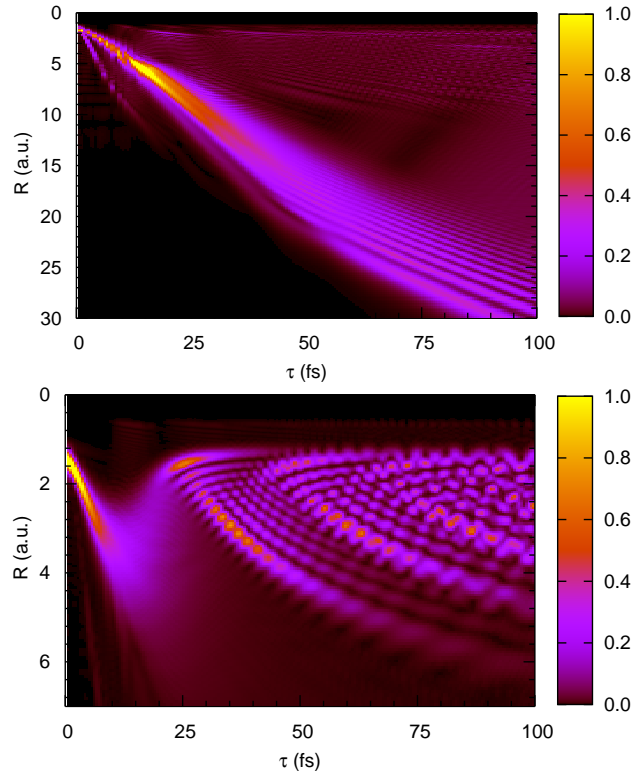


Figure 10: Time-dependence of the distribution of the vibrational wave packet on the σ_u (upper panel) and σ_g (lower panel) potential surfaces of D_2^+ molecular ions after the initial ionization of D_2 by an 8 fs pulse. Time is measured from the peak of the laser pulse.

and also splitting, due to the interference of the different components of the wave packet.

The wave packet that is riding on the bound ground σ_g potential shows surprisingly complicated time evolution. In the first half cycle, this wave packet simply moves outward to larger R , with a bit of spreading. Within the next half vibrational period, this wave packet does not return as a recognizable localized wave packet. At each instant, the wave packet is quite spread out. As the time goes on, the wave packet gradually rebuilds itself near the inner classical turning point. After about one vibrational period, it begins its outward journey again, albeit with a slower mean velocity. In the meanwhile, small interference peaks are clearly seen, resulting from the two oppositely travelling wave packets within the σ_g potential. Clearly the figure shows that the wave packet that is riding on the bound potential curve is highly nonclassical, and has complicated interference structures.

How the theoretical simulation for the wave packet dynamics be probed

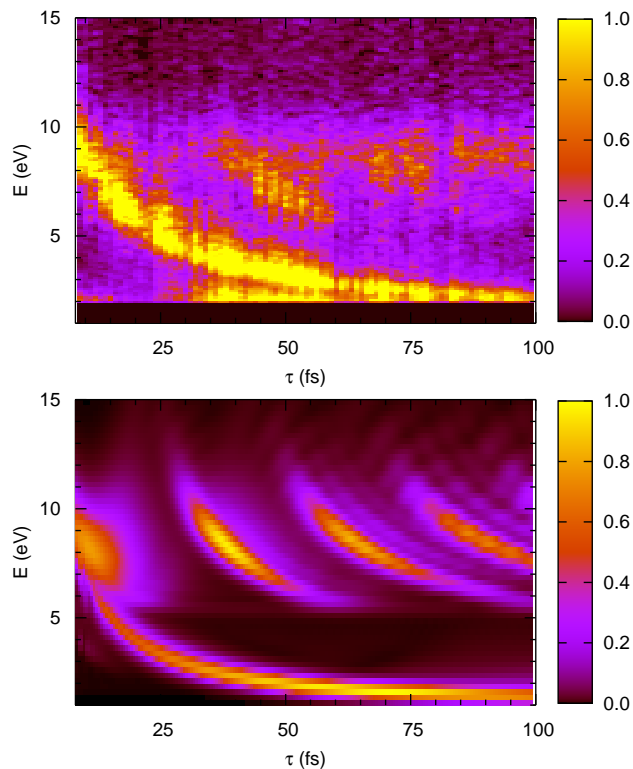


Figure 11: Kinetic energy release spectra of D^+ ions as a function of time delay between the pump and probe lasers from theoretical simulation (lower panel) and experimental measurement (upper panel). The pulse width of each laser is 8 fs and the peak intensity is 3×10^{14} W/cm² for the pump laser and 8×10^{14} W/cm² for the probe laser.

experimentally? With the present-day laser technology, this is most easily done by using a coherent probe laser with sufficient range of time delay to ionize the D_2^+ ion. Such an experiment has been carried out at Kansas State University recently [33]. After the initial pump with an 8 fs pulse with peak intensity of 3×10^{14} W/cm², an intense 8 fs probe pulse with higher peak intensity 8×10^{14} W/cm² was used to ionize the D_2^+ ion. This intensity is strong enough to fully ionize the D_2^+ ion if it is in the excited state. It can ionize the D_2^+ ion with probability of the order of 0.1 if the ion is in the ground electronic state, and if the internuclear distance is about 4 a.u. or higher. In other words, the portion of the wave packet associated with the σ_g potential curve can be probed directly if the wave packet has significant distribution in the region larger than 4 a.u. After ionization, the kinetic energy from the Coulomb explosion identifies the internuclear separation where the ionization occurs.

In Fig. 11, the experimental kinetic energy release from the Coulomb explo-

sion is displayed vs the time delay. The stripes of islands of peaks near 6-10 eV clearly can be identified with wave packet associated with the ground potential curve. There is no indication of the "reflecting" wave packet, in agreement with the simulated wave packet. The single long low energy streak at decreasing kinetic energy clearly indicates that it is the result of ionization from the upper repulsive σ_u potential curve. The kinetic energy release decreases since the ionization occurs at larger internuclear distances with increasing time delay. The experimental results can be compared to the calculated kinetic energy spectra obtained from the theoretical simulation. The agreement between the simulation and the experimental data is very good, supporting the assertion that the wave packet motion is not classical in nature.

There are at least two lessons learned from this elementary experimental study. First, the wave packet dynamics in general is not very classical. Besides the general broadening, the wave packet can undergo major distortion, in regions near classical reflections and in regions where coupling to other channels becomes important. Second, the wave packet can be probed or modified in ways depending strongly on the second laser or light source. Using 8 fs laser pulse of moderate intensity of 8×10^{14} W/cm², only the wave packet in the outer region (or larger internuclear separations) can be probed or modified. In other words, the snapshot by the probe pulse did not map out the whole wave packet. To map out the whole wave packet, or to modify the whole packet significantly, one would need to have a photon source with broad energy band. This is achievable only with attosecond pulses with mean wavelength in the extreme ultraviolet regime. Clearly a "movie" made out of attosecond pulses would see the whole wave packet that cannot be achieved with present-day femtosecond pulses.

5 Summary and Discussion

In this article, we have selected three examples to show how insightful information on the structure and the dynamics of simple molecules can be probed using short intense laser pulses. In the first example, we show that by properly choosing laser pulse intensity and duration, the angular distribution of the fragments of ions following the double ionization of molecules can be used to map out directly the geometry (or shape) of the elementary molecular orbitals. Essential to this mapping is the fact that in tunneling ionization the ionization rate is proportional to the electron density in the direction of the laser polarization. By rotating the internuclear axis, one maps out the electron density in the direction of the laser polarization and thus the tunneling ionization rates. We emphasized that sub-10 fs laser pulses are essential and proper laser intensity is needed for such mapping. In the second example, we studied the time sequence of the double ionization of H₂ or D₂ molecules. After the initial ionization by the laser, we showed that the second ionization can occur either by the returning rescattering electron, or by the succeeding peak fields of the laser. The times for rescattering and for sequential ionization are tied directly to the laser's optical period. Thus double ionization can occur at well defined

time intervals and these time intervals can be measured experimentally from the kinetic energy release of the double ionization fragments. By changing the laser intensity and/or the pulse length, the relative importance of these ionization events can be controlled. Thus the time interval between the two ionization events can be controlled and can be determined. This forms the idea of the molecular clock where time can be measured accurately to less than 1 fs. In the third example, we show how to probe simple wave packet dynamics. The wave packet was generated by first ionizing the ground state of H_2 and probed by another short laser pulse after a sequence of time delays. The propagation of the wave packet in the laser field undergoes additional coupling, resulting in the splitting of the wave packet, and subsequently, the wave packet is riding on two potential surfaces. The motion of these two correlated wave packets can be probed simultaneously by another probe laser. The results shows that the wave packets are highly nonclassical. We have shown that to map out the whole wave packet, XUV attosecond pulses would be needed in the future.

In this article, we have shown new insights of the dynamics of molecules have been revealed with the availability of new Ti-Sapphire lasers with pulse durations of less than 10 fs. As the laser pulses are being pushed to shorter durations, to attosecond pulses, and to different mean wavelengths, the tools available to the experimentalists are to increase significantly. By using these different tools, one day the reaction dynamics and its pathway can be controlled completely by the experimentalists. On the other hand, without theoretical guidance progress would be greatly hampered in view of the large number of parameters that the experimentalists have to face.

This work was supported in part by Chemical Sciences, Geosciences and Biosciences Division, Office of Basic Energy Sciences, Office of Science, U. S. Department of Energy.

References

- [1] J. Ullrich, R. Moshhammer, R. Dorner, O. Jagutzki, V. Mergel, H. Schmidt-Böcking, and L. Spielberger, *J. Phys. B* **30**, 2917 (1997).
- [2] R. Dörner, V. Mergel, O. Jagutzki, L. Spielberger, J. Ullrich, R. Moshhammer, and H. Schmidt-Böcking, *Phys. Rep.* **330**, 95 (2000).
- [3] L. J. Frasinski, K. Codling, P. Hatherly, J. Barr, I. N. Ross, and W. T. Toner, *Phys. Rev. Lett.* **58**, 2424 (1987).
- [4] D. T. Strickland, Y. Beaudoin, P. Dietrich, and P. B. Corkum, *Phys. Rev. Lett.* **68**, 2755 (1992).
- [5] C. Guo, M. Li, J. P. Nibarger, and G. N. Gibson, *Phys. Rev. A* **61**, 033413 (2000).
- [6] H. Stapelfeldt and T. Seideman, *Rev. Mod. Phys.* **75**, 543, (2003).

- [7] A. S. Alnaser, S. Voss, X. M. Tong, C. M. Maharjan, P. Ranitovic, B. Ulrich, T. Osipov, B. Shan, Z. Chang, and C. L. Cocke, *Phys. Rev. Lett.* **93**, 113003, (2004).
- [8] S. Voss, A. S. Alnaser, X. M. Tong, C. Maharjan, P. Ranitovic, B. Ulrich, B. Shan, Z. Chang, C. D. Lin, and C. L. Cocke, *J. Phys. B* **37**, 4239 (2004).
- [9] X. M. Tong, Z. X. Zhao, A. S. Alnaser, S. Voss, C. L. Cocke, and C. D. Lin, *J. Phys. B* **38**, 333 (2005).
- [10] A. S. Alnaser, C. M. Maharjan, X. M. Tong, B. Ulrich, P. Ranitovic, B. Shan, Z. Chang, C. D. Lin, C. L. Cocke, and I. V. Litvinyuk, *Phys. Rev. A* **71**, 031403 (2005).
- [11] X. M. Tong, Z. X. Zhao, and C. D. Lin, *Phys. Rev. A* **66**, 033402 (2002).
- [12] L. D. Landau and E. M. Lifshitz, *Quantum mechanics : non-relativistic theory* (Pergamon Press, New York, 1977).
- [13] M. V. Ammosov, N. B. Delone, and V. P. Krainov, *Zh. Eksp. Teor. Fiz.* **91**, 2008 (1986), [*Sov. Phys. JETP* **64**,1191 (1986)].
- [14] M. W. Schmidt, K. K. Baldridge, J. A. Boatz, S. T. Elbert, M. S. Gordon, J. J. Jensen, S. Koseki, N. Matsunaga, K. A. Nguyen, S. Su, *et al.*, *J. Comput. Chem.* **14**, 1347 (1993).
- [15] S. Portmann and H. P. Lüthi, *CHIMIA* **54**, 766 (2000).
- [16] A. H. Zewail, *J. Phys. Chem. A* **104**, 5660 (2000).
- [17] H. Niikura, F. Legare, R. Hasbani, A. D. Bandrauk, M. Y. Ivanov, D. M. Villeneuve, and P. B. Corkum, *Nature* **417**, 917 (2002).
- [18] H. Niikura, F. Legare, R. Hasbani, M. Y. Ivanov, D. M. Villeneuve, and P. B. Corkum, *Nature* **421**, 826 (2003).
- [19] T. Zuo and A. D. Bandrauk, *Phys. Rev. A* **52**, R2511 (1995).
- [20] K. Codling, L. J. Frasinski, and P. A. Hatherly, *J. Phys. B* **22**, L321 (1989).
- [21] T. Seideman, M. Y. Ivanov, and P. B. Corkum, *Phys. Rev. Lett.* **75**, 2819 (1995).
- [22] E. Constant, H. Stapelfeldt, and P. B. Corkum, *Phys. Rev. Lett.* **76**, 4140 (1996).
- [23] A. Giusti-Suzor, F. H. Mies, L. F. DiMauro, E. Charron, and B. Yang, *J. Phys. B* **28**, 309 (1995).
- [24] K. Codling and L. J. Frasinski, *J. Phys. B* **26**, 783 (1993).
- [25] A. Bandrauk, *Comments At. Mol. Phys.* **1 D**, 97 (1999).

- [26] A. S. Alnaser, X. M. Tong, T. Osipov, S. Voss, C. M. Maharjan, P. Ranitovic, B. Ulrich, B. Shan, Z. Chang, C. D. Lin, and C. L. Cocke, Phys. Rev. Lett. **93**, 183202 (2004).
- [27] X. M. Tong, Z. X. Zhao, and C. D. Lin, Phys. Rev. A **68**, 043412, (2003).
- [28] X. M. Tong, Z. X. Zhao, and C. D. Lin, Phys. Rev. Lett. **91**, 233203, (2003).
- [29] G. L. Yudin and M. Y. Ivanov, Phys. Rev. A **64**, 035401 (2001).
- [30] I. Bray, <http://atom.murdoch.edu.au/CCC-WWW/index.html>.
- [31] X. M. Tong and C. D. Lin, Phys. Rev. A **70**, 023406, (2004).
- [32] K. Sandig, H. Figger, and T. W. Hansch, Phys. Rev. Lett. **85**, 4876 (2000).
- [33] A. S. Alnaser, *et al.*, **in press** (2005).